

The Redshift and Real-Space Correlation Functions from the ESP Galaxy Redshift Survey

L. Guzzo¹, J.G. Bartlett², A. Cappi³, S. Maurogordato⁴, E. Zucca³, G. Zamorani^{3,5}, C. Balkowski⁶, A. Blanchard², V. Cayatte⁶, G. Chincarini^{1,7}, C.A. Collins⁸, D. Maccagni⁹, H. MacGillivray¹⁰, R. Merighi³, M. Mignoli³, D. Proust⁶, M. Ramella¹¹, R. Scaramella¹², G.M. Stirpe³, G. Vettolani⁵

¹*Osservatorio Astronomico di Brera, I-23807 Merate, Italy*

²*Université L. Pasteur, Obs. Astronomique, F-67000 Strasbourg, France*

³*Osservatorio Astronomico di Bologna, I-40126 Bologna, Italy*

⁴*Observatoire de Nice, B4229, F-06304 Nice Cedex 4, France*

⁵*Istituto di Radioastronomia del CNR, I-40129 Bologna, Italy*

⁶*Observatoire de Paris, DAEC, F-92195 Meudon, France*

⁷*Università degli Studi di Milano, I-20133 Milano, Italy*

⁸*Liverpool John-Moores University, Liverpool L3 3AF, UK*

⁹*Istituto di Fisica Cosmica e Tecnologie Relative del CNR, I-20133 Milano, Italy*

¹⁰*Royal Observatory Edinburgh, Edinburgh EH9 3HJ, UK*

¹¹*Osservatorio Astronomico di Trieste, I-34131 Trieste, Italy*

¹²*Osservatorio Astronomico di Roma, I-00040 Monteporzio Catone, Italy*

Abstract. We discuss the behaviour of the redshift- and real-space correlation functions from the ESO Slice Project (ESP) galaxy redshift survey. $\xi(s)$ for the whole survey is positive out to $\sim 80 \text{ h}^{-1} \text{ Mpc}$, with a smooth break from a power law. By projecting $\xi(r_p, \pi)$, we recover the real-space correlation function $\xi(r)$, which below $10 \text{ h}^{-1} \text{ Mpc}$ is reasonably well described by a power law $\xi(r) = (r/r_0)^{-\gamma}$, with $r_0 = 4.15^{+0.20}_{-0.21} \text{ h}^{-1} \text{ Mpc}$ and $\gamma = 1.67^{+0.07}_{-0.09}$. The same analysis, applied to four volume-limited subsamples, evidences a small but significant growth of clustering with luminosity (r_0 varies from 3.4 to $5.2 \text{ h}^{-1} \text{ Mpc}$, when the luminosity threshold is increased from -18.5 to -20).

1 The ESP Survey

The original goal of the ESO Slice Project (ESP) redshift survey was essentially twofold. First, we wanted to produce a measure of the galaxy luminosity function in the “local” ($z < 0.2$) Universe, with large dynamic range. Second, we wanted to study the clustering of galaxies from a survey hopefully not dominated by a single major superstructure, as it was the case for the surveys available at the beginning of this decade. While the ESP luminosity function and its implications are discussed in detail in [11] and summarised also in these proceedings by Elena Zucca, here we shall summarise our results on the two-point correlation properties of galaxies.

The ESP survey covers a strip of sky 1° thick (DEC) by $\sim 30^\circ$ long (RA)

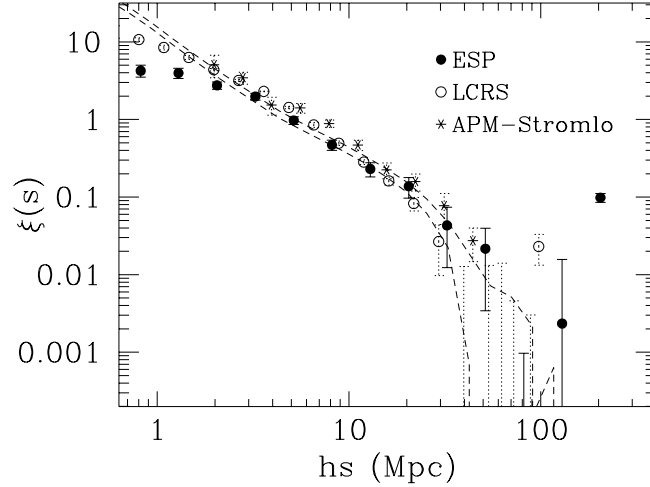


Figure 1: The redshift-space correlation function from the whole ESP magnitude-limited catalogue, compared to previous data (see text).

(with an unobserved 5° sector inside this strip), in the SGP region. The target galaxies were selected from the EDSGC [3], and the final catalogue contains 3342 redshifts, corresponding to a completeness of 85% at a magnitude limit $b_J = 19.4$ [10]. We use $H_o = 100 \text{ km s}^{-1} \text{ Mpc}^{-1}$ and $q_o = 0.5$. Magnitudes are K-corrected as described in [11].

2 Clustering in Redshift Space

The filled circles in Figure 1 show $\xi(s)$ computed from the whole ESP magnitude-limited sample using the J3-weighting technique, (e.g. [2]). Note the smooth decay from the power law at large separations, with correlations going to zero only around $80 \text{ h}^{-1} \text{ Mpc}$, and perhaps some evidence for a positive fluctuation around $\sim 200 \text{ h}^{-1} \text{ Mpc}$. Below $\sim 3 \text{ h}^{-1} \text{ Mpc}$, $\xi(s)$ tends to flatten. This is the effect of redshift-space damping from pairs within virialized structures and interestingly it is less prominent when $\xi(s)$ is computed for volume-limited subsamples [5]. In the same figure, we show $\xi(s)$ from the Las Campanas (LCRS, [8]), and APM-Stromlo [7] redshift surveys. There is a rather good agreement of the three independent data sets between 2 and $20 \text{ h}^{-1} \text{ Mpc}$ (where $\xi(s) = (s/s_o)^{-\gamma}$, with $s_o \sim 6 \text{ h}^{-1} \text{ Mpc}$ and $\gamma \sim -1.5$), with perhaps a hint for more power on larger scales in the blue-selected ESP and APM-Stromlo. In addition, the dashed lines describe the real-space $\xi(r)$ obtained by deprojecting the angular correlation function $w(\theta)$ of the APM Galaxy Catalogue [1], for two different assumptions on the evolution of clustering. It is

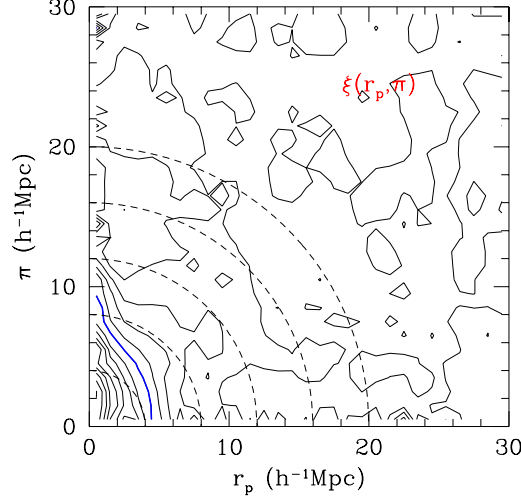


Figure 2: $\xi(r_p, \pi)$ contour map for the whole ESP survey. The heavy contour corresponds to $\xi = 1$.

rather interesting to note the degree of unanimity between the angular and redshift data in indicating both the large-scale shape and the zero-crossing scale ($40 - 90 \text{ h}^{-1} \text{ Mpc}$) of galaxy correlations. The small amplitude difference between the redshift and real-space correlations on scales $> 5 \text{ h}^{-1} \text{ Mpc}$ is also remarkable, because it suggests a small amplification of $\xi(s)$ due to streaming flows, and thus a low value of $\beta = \Omega_o/b$.

3 Clustering in Real Space

Redshift distortions produced by peculiar velocities, are usually studied through the function $\xi(r_p, \pi)$ [4], that describes galaxy correlations as a function of two variables, one perpendicular (r_p), and the other parallel (π), to a sort of mean line of sight defined for each galaxy pair. In Figure 2, we show $\xi(r_p, \pi)$ computed for the whole ESP survey, using the same technique used for $\xi(s)$. From this figure, one can clearly see the small-scale stretching of the contours along π , produced by the relative velocity dispersion of pairs within structures. Projecting $\xi(r_p, \pi)$ onto the r_p axis, one gets the function $w_p(r_p)$, which is independent from the redshift-distortion field, and is analytically integrable for a power-law $\xi(r) = (r/r_o)^{-\gamma}$. In this case, the values of r_o and γ that best reproduce the data can be evaluated through an appropriate best-fitting procedure. By applying this to the map of Figure 2, we recover $r_o = 4.15^{+0.20}_{-0.21} \text{ h}^{-1} \text{ Mpc}$ and $\gamma = 1.67^{+0.07}_{-0.09}$, a value that is slightly smaller than that measured from the red-selected LCRS [6]. Finally, we have investigated the stability of $\xi(r)$ as a function of the sample mean luminosity, by computing $w_p(r_p)$ for

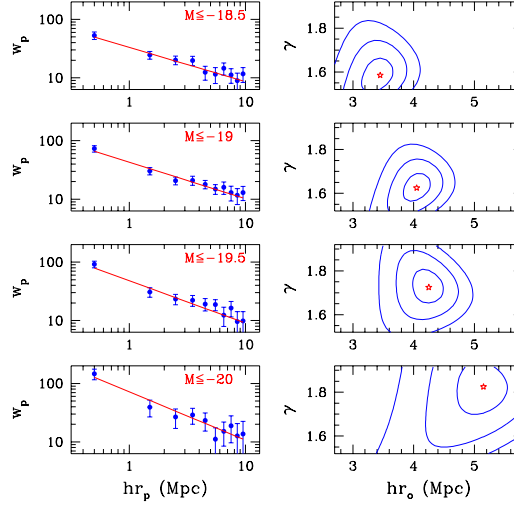


Figure 3: Fits of a power-law $\xi(r)$ to $w_p(r_p)$ for four volume-limited samples.

four volume-limited subsamples. Figure 3 shows the result of the power-law fit to $w_p(r_p)$, evidencing a weak, but significant growth of r_0 and γ when more and more luminous galaxies are selected. Interestingly, this behaviour is completely masked if one looks at $\xi(s)$ [5], the reason being the rather different small-scale distortion acting in the four cases, that basically compensates the (real-space) growth of clustering. This shows the importance of separating out dynamical effects when comparing the clustering of different classes of objects through the two-point correlation function.

References

- [1] Baugh, C.M., 1996, MNRAS 280, 267
- [2] Fisher, K.B., Davis, M., Strauss, M.A., Yahil, A., & Huchra, J.P. 1994a, MNRAS, 266, 50 (F94a)
- [3] Heydon-Dumbleton, N.H., Collins, C.A., MacGillivray, H.T., 1989, MNRAS 238, 379
- [4] Guzzo, L., Strauss, M.A., Fisher, K.B., Giovanelli, R., and Haynes, M.P. 1997, ApJ, 489, 37
- [5] Guzzo, L., et al. (The ESP Team), 1998a, A&A, submitted
- [6] Lin, H., 1995, PhD Thesis, Harvard University
- [7] Loveday, J., Peterson, B. A. Maddox, S. J., Efstathiou, G., 1996, ApJ Suppl. 107, 201
- [8] Schectman, S.A., Landy, S.D., Oemler, et al., 1996, ApJ 470, 172
- [9] Vettolani, G., et al. (the ESP Team), 1997, A&A 325, 954
- [10] Vettolani, G., et al. (the ESP Team), 1998, A&A Suppl., 130, 323
- [11] Zucca, E., et al. (the ESP Team), 1997, A&A, 326, 477